DNA-tile structures lead to ionic currents through lipid membranes

Kerstin Göpfrich,[†,¶] Thomas Zettl,[†,‡,¶] Anna E. C. Meijering,[†] Silvia Hernández-Ainsa,[†] Samet Kocabey,[‡] Tim Liedl,[‡] and Ulrich F. Keyser [*,†]

Cavendish Laboratory, University of Cambridge, Cambridge CB3 0HE, United Kingdom, and Center for NanoScience and Department of Physics, Ludwig-Maximilians-Universität München, 80539 München, Germany

E-mail: ufk20@cam.ac.uk

Phone: +44(0)1223 337272

[*]To whom correspondence should be addressed
[†]University of Cambridge
[‡]Ludwig-Maximilians-Universität München
[¶]These two authors contributed equally to this work.

Abstract

Self-assembled DNA nanostructures have been used to create man-made transmembrane channels in lipid bilayers. Here, we present a DNA-tile structure with a nominal sub-nanometer channel and cholesterol-tags for membrane anchoring. With an outer diameter of 5 nm and a molecular weight of 45 kDa, the dimensions of our synthetic nanostructure are comparable to biological ion channels. Due to its simple design, the structure self-assembles within a minute, making its creation scalable for applications in biology. Ionic current recordings demonstrate that the tile structures enable ion conduction through lipid bilayers and show gating and voltage-switching behaviour. By demonstrating the design of DNA-based membrane channels with openings much smaller than that of the archetypical six-helix bundle, our work showcases their versatility inspired by the rich diversity of natural membrane components.

KEYWORDS: DNA nanotechnology, artificial ion channels, DNA-tiles, single-molecule, lipid bilayer, self-assembly

The transport of ions across lipid membranes is essential for a wide range of vital biological processes including signal transduction in electrically excitable tissue.[1] There have been ongoing efforts to create synthetic channels inspired by their biological counterparts.[2–4] Such artificial constructs can advance our fundamental understanding of the physical principles dictating functions of ion channels in cells, serve as tailored biosensors,[5] cytotoxic agents[6] or drug carriers.[7]

Nanopores entirely constructed of DNA have been introduced as a versatile tool for single-molecule sensing.[8–10] Their incorporation into lipid membranes was another important step towards synthetic DNA-based ion channels.[11–14] In order to allow for the insertion of the charged DNA structure into the lipid bilayer, hydrophobic tags like cholesterol,[11] porphyrin[12] and ethane-PPT groups[13] were strategically positioned on the channels. While the DNA origami technique[15] was employed to construct pores with a molecular weight of over 2000 kDa,[11] DNA nanotechnology also enables the creation of pores with lower molecular weights comparable to those of biological ion channels.

Here, we use DNA tiles[16,17] as an alternative approach for the creation of DNA-based membrane channels. Due to their simple design, our structures can readily be made within a minute at micro molar concentrations and high yields avoiding complex heating protocols. Additionally, our design prototypes a novel architecture. It consists of only four helices on a square lattice, whereas all previously presented DNA membrane channels are based on a bundle of six DNA duplexes arranged on a honeycomb lattice.[11–14] We thus reduced the nominal channel width from 2 nm to 0.8 nm, reaching typical diameters of ion channels.[1] Our simple design will inform the design pathway towards DNA-based membrane pores beyond the current use for biosensing opening up broad perspectives for the development of their biotechnological and biomedical applications.[7,18]

Our DNA-tile structure consists of four 11 nm long DNA duplexes arranged on a square lattice as illustrated in Figure 1 A. In this arrangement, the naturally emerging gap between the helices gives rise to a central channel with a nominal diameter of 0.8 nm, assuming

geometrical packing and an anhydrated helix diameter of 2 nm. The duplexes are formed from eight interconnected single-stranded DNA tiles two of which carry terminal cholesterol modifications to allow for membrane anchoring. The exact sequence of the tiles is shown in the Supplementary Information (Table S1). Two additional tiles carry Cy3-tags for visualisation by fluorescence microscopy. The pathways of the tiles and their two crossovers per neighbouring helix are shown in Figure 1 B. Terminal adenine repeats were introduced at both ends of the structure to avoid stacking of multiple structures.[17] While one end of the structure was stabilised with terminal crossovers for optimal membrane insertion (Figure 1 B, right end), the other end was left open (left end). Fluctuations are enhanced further due to the short length of the tiles and the symmetric crossover positions. Our design aims to mimic the complex behaviour of biological ion channels by increasing the structural flexibility and reducing the diameter to the molecular scale, as opposed to previous DNA membrane structures with larger diameters that were primarily created for biosensing applications.[11,14]

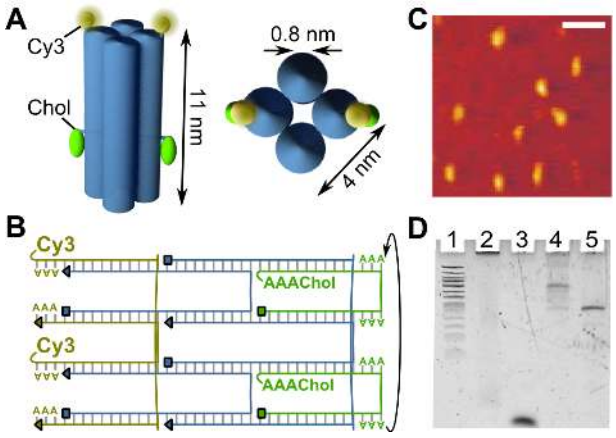

Figure 1: Schematic side view (left) and top view (right) of the DNA-tile structure composed of four interconnected duplexes represented as cylinders. The two cholesterol-anchors are shown in green, the Cy3-tags in yellow. B) Pathways of the eight tiles forming the four duplexes and positions of the Cy3 and cholesterol modifications. Squares represent the 5' ends, triangles the 3' ends, base pairs are indicated as vertical bars. C) AFM image (tapping mode) of the DNA-tile structure. Scale bar: 100 nm. D) 10% Polyacrylamide gel electrophoresis. Lane 1: 50 bp DNA ladder; Lane 2: Complete DNA-tile structure with two cholesterol-tags; Lane 3: Individual ssDNA strand (28 bp); Lane 4: Complete DNA-tile structure without cholesterol-tags; Lane 5: DNA-tile structure missing the two cholesterol-tagged strands.

The DNA-tile structure was assembled by annealing equimolar concentrations of the six cholesterol-free tiles at a final concentration of 1 μM in 10 mM Tris-HCl, 1 mM EDTA, 20 mM $MgCl_2$, pH 8.0. Subsequently, the two cholesterol-tagged tiles were added in 5× excess at room temperature (RT). The structure was characterised to probe its correct assembly. Atomic force microscopy (AFM) confirmed the monomeric nature and established that the dimensions fell within the expected bounds for such a small design (Figure 1 C). Polyacrylamide gel electrophoresis without the cholesterol-tagged tiles yields a single band (Figure 1 D, Lane 5), whereas the migration in the gel of structures with the cholesterol tiles is most likely hindered by hydrophobic interactions (Lane 2). This demonstrates that the cholesterol-modified DNA strands are successfully incorporated. As expected, a fully assembled design with all eight tiles but no cholesterol-tags migrates slower than the six-tile construct (Lane 4). Dynamic light scattering (DLS) gives further indication of the monomeric nature and reasonable size of both the construct missing the cholesterol-modified tiles (hydrodynamic radius: 5.1 nm) and the complete structure with cholesterol (hydrodynamic radius: 7.8 nm, see SI, Figure S1).

A major advantage of our tile-based design is its simplicity resulting in minimal preparation time and a significant cost reduction (for details see SI, Table S3). Additionally, the use of long annealing protocols becomes redundant. We assembled the six-tile construct lacking the two cholesterol-modified tiles in 10 mM Tris-HCl, 1 mM EDTA, 20 mM $MgCl_2$, pH 8.0 using four different assembly protocols:

1. An 18 hour long standard annealing protocol (heating to 80 °C for 5 min, cooling down to 65 °C using a linear cooling ramp over 75 min, subsequently cooling to 25 °C within 16 hours) as a benchmark procedure;

2. A 10 min thermocycler protocol (heating to 80 °C for 5 min, holding at 65 °C for 5 min);

3. A 10 min water-bath treatment (80 °C);

4. A 10 min incubation at room temperature (RT).

To assess the feasibility and assembly yield for each protocol, we performed polyacrylamide gel electrophoresis as shown in Figure 2 A. We confirm that the structure has successfully been formed under all assembly conditions. The intensity of the bands is indicative of the obtained yield. Notably, the 10 min annealing (Protocol 2) still yields 85% compared to the benchmark conditions (Protocol 1). The Protocols 3 and 4 without thermocycler result in 78% and 76% respectively. To estimate the required assembly time for our construct, we performed UV-melting experiments. Figure 2 B shows a single sharp transition from the low absorption of the double-stranded species to the high absorption of the single strands at a melting temperature of 63 °C. This demonstrates the correct assembly. Subsequently, the single-stranded sample was cooled at a rate of 5 °C/min to allow for re-hybridisation. The shift in melting temperature is proportional to the required assembly time. At the given cooling rate, the observed shift of 8 °C effectively corresponds to an upper limit of 2 min for the folding time. The fact that the absorption returns to its original value after the temperature cycle indicates that the number of correctly assembled structures remains at a similar level even for such short duration of the programme. It should be noted that the heating rate has to be reduced to obtain a more accurate estimation of the melting point. At a rate of 0.25 °C/min, the melting transition lies at 53 °C (see SI, Figure S2). If the UV-melting experiments are performed in the presence of giant unilamellar vesicles (GUVs, lipid composition: DPhPC, 10% cholesterol), the melting temperature of the fully assembled structure with cholesterol anchors increases by approximately 5 °C (see SI, Figure S2). This thermal stabilisation can be explained through a considerable interaction between GUVs and our DNA-tile structures, as it is not observed in the absence of cholesterol-tags. Similar observations have been made by Burns *et al.* for different hydrophobic anchors.[12]

Finally, fluorescent confocal imaging was carried out to visualise the interaction of the DNA-tile structure with GUVs. Using this technique, we could demonstrate that the com-

plete structure with cholesterol-anchors assembles and attaches to GUVs within a minute. A mixture of all eight tiles was kept at 80 °C to prevent hybridisation before adding the sample to GUVs at RT. Figure 2 C shows a GUV imaged in bright field (left) and fluorescence mode (middle) directly after addition of the sample containing the DNA-tile structures. After only 60 sec, a bright ring around the same GUV (right) indicates the presence of DNA-tile structures on the membrane of the vesicle. This proves that the DNA assembly was complete, since only a fully formed structure connects both the Cy3-tag and the cholesterol-tag (see Figure 1 B). Control experiments show that membrane attachment requires the presence of at least one cholesterol-anchor (see SI, Figure S4). The uniform distribution of DNA-tile structures around the GUV points towards minimal aggregation. Even though larger aggregates are sometimes visible in the fluorescent images, especially after long storage of the sample, we observed that aggregation is significantly reduced upon addition of GUVs (see SI, Figure S6 and S7). Interestingly, high concentrations of DNA-tile structures led to the formation of tubular lipid deformations as shown in Figure 2 D (left). Two lipid compositions were tested, DOPC (see Figure 2 D) and DPhPC with 10% cholesterol (see SI, Figure S5), which both exhibit these deformations. Similar observations were previously made for high concentrations of certain membrane-binding proteins.[19,20] Crowding of DNA structures on the membrane could lead to increased pressure. This might help to overcome the energy barrier for bending of the membrane as has been proposed for specialised membrane proteins.[19] Alternatively, our DNA-tile structures could behave like amphiphilic membrane-inserted α-helices that are hypothesised to cause membrane bending.[20] To test if the tubular structures are indeed lipid deformations rather than aggregates of our DNA-tile structures, we prepared a sample without Cy3-tags and added it to GUVs containing fluorescently labelled lipids (DOPC, 1% NBD-DPhPE). The confocal image in Figure 2 D (middle) confirms the hypothesis of lipid deformation. Importantly, addition of high concentrations of cholesterol-tagged ssDNA alone does not cause membrane bending (Figure 2 D, right).

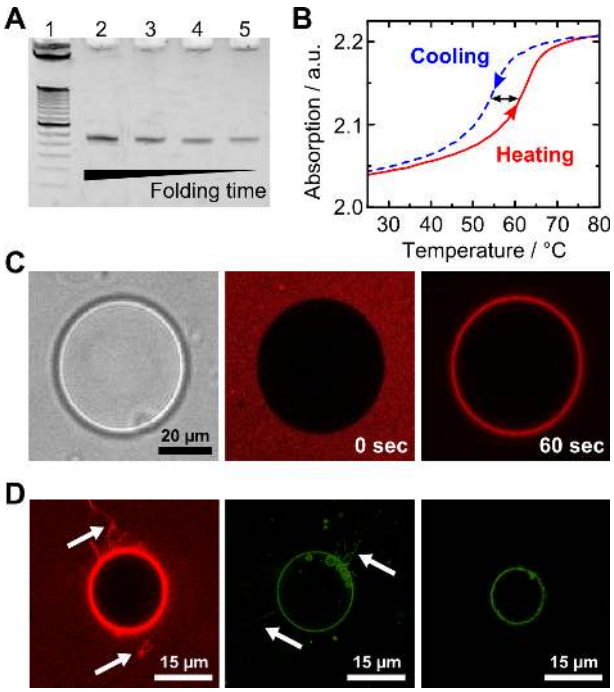

Figure 2: A) 10% polyacrylamide gel electrophoresis. Lane 1: 50 bp DNA ladder; Subsequent lanes: DNA-tile structure lacking the two cholesterol-modified tiles annealed for 18 h in the thermocycler (Lane 2), for 10 min in the thermocycler (Lane 3), for 10 min in a hot water bath (Lane 4) and for 10 min at RT (Lane 5). B) Absorption measured at 260 nm during a heating (red) and a subsequent cooling cycle (blue). At the cooling rate of 5 °C/min the shift in melting temperature gives an upper limit for the folding time of 2 min. C) Giant unilamellar vesicle (GUV) imaged in bright field (left) and fluorescence mode (excitation: 514 nm). 60 sec after addition of the ssDNA-tile mixture, a bright ring forms around the vesicle, indicating rapid folding and membrane attachment of the structure. D) Left: Addition of high concentrations of fluorescent DNA-tile structures leads to formation of tubular structures on GUVs; Middle: GUVs formed from fluorescently labelled lipids with high concentrations of non-fluorescent DNA-tile structures; Right: cholesterol-tagged ssDNA only.

This study was set out to investigate whether DNA-tiles can be used for the efficient creation of ion channel-like structures. Since fluorescent imaging confirmed that the DNA-tile structures strongly interact with lipid vesicles, we decided to form lipid bilayers for electro-physiological characterisations directly from these vesicles. We use our lipid nano bilayer system[14,21,22] which allows us to screen large numbers of vesicles for the incorporation of pores relatively quickly. We incubated GUVs (DPhPC, 10% cholesterol) with DNA-tile structures in 1 M KCl, 10 mM MES, pH 6.0. As illustrated in Figure 3 A, these vesicles were then suctioned onto the tip of a 200 nm diameter glass capillary (1), where they burst and form a bilayer. This bilayer is then subjected to a standardised current-voltage (IV)-recording protocol (2), before it is removed from the capillary by applying a positive pressure (3). We repeated this process at least 100 times for each of the experimental conditions to obtain reasonable statistics. All GUVs are tested without DNA-tile structures first to assess bilayer quality. The GUVs are only used for recordings if they have a consistent conductance in the range of tens of pS and no pore-like events are observed. Figure 3 B shows the conductances of 170 independent IV-recordings for plain GUVs (top) and GUVs that have been incubated with DNA-tile structures (bottom). None of the bilayers formed from plain GUVs show a conductance above 0.3 nS. In contrast, 12% of bilayers formed from GUVs with DNA structures exhibit conductances well above. It is also important to note that the percentage of bilayers with conductances between 0.15 nS and 0.3 nS increases. Control experiments were carried out with GUVs that were incubated with the cholesterol-modified ssDNA only, with DNA-tile structures without cholesterol anchors, with a cholesterol-tagged DNA duplex, with only one cholesterol-anchor and with four cholesterol-anchors. The percentage of bilayers with conductances above 0.15 nS for each of these conditions is much higher in the presence of DNA-tile structures with two or four cholesterol-anchors (see SI, Table S2). This clearly demonstrates that only our fully assembled DNA-tile structures are capable of producing ion conduction in lipid membranes.

However, an increase in ion conduction is not the only way in which bilayers holding

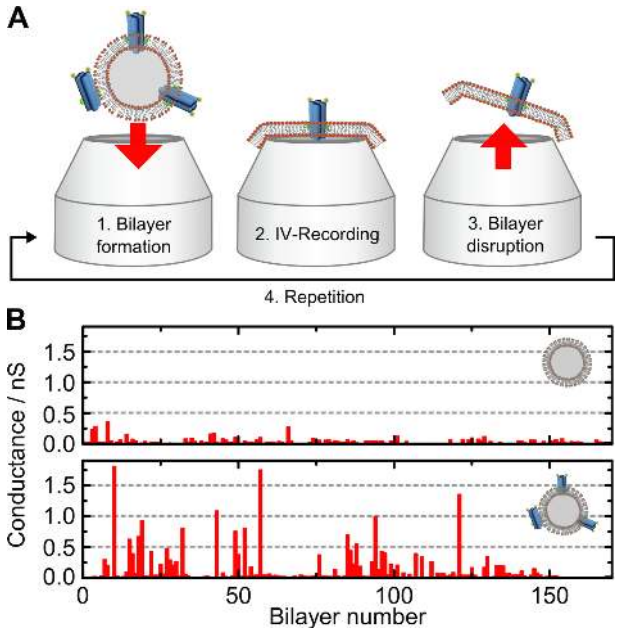

Figure 3: A) Illustration of the ionic current measurement protocol on our lipid nano bilayer setup. The same protocol was used for GUVs without DNA-tile structures. B) Conductances obtained for 170 independent IV-recordings of GUVs without (top) and with DNA-tile structures (bottom).

functional tile structures are distinct from plain bilayers. We observe characteristic events that we can attribute to the presence of one or more DNA-tile assemblies, like a stepwise increase or decrease in current at constant voltage. A typical event is shown in Figure 4 A. It is likely to correspond to flipping of a DNA-tile structure that was previously bound to the membrane into an ion conducting orientation.

Additionally, we often observe gating as shown in Figure 4 B. In Figure 4 C, we present typical ionic current traces obtained from IV-recordings in the presence of DNA-tile structures with cholesterol-anchors. A rigid cylindrical channel with the nominal diameter of 0.8 nm has an estimated conductance of 0.47 nS in 1 M KCl. However, the effective channel diameter in solution is expected to deviate from the nominal value. The hydrodynamic helical diameter has been estimated as 2.2 to 2.6 nm[23] (compared to 2 nm anhydrated) and electrostatic repulsion between the helices can increase the effective channel diameter further.[24–26] On the other hand, the diameter of a membrane-embedded structure may be reduced due to

lateral membrane pressure. In line with our data, rigid channels with a uniform conductance are not expected at near-molecular length scales. Although we sometimes obtain ohmic current traces (black), traces with reduced conductance at higher voltage (green) are very characteristic. It is interesting to note here that comparable gating and voltage-switching behaviour has also been reported for the archetypal six-helix bundle in both planar bilayers and lipid nano bilayers.[14] Despite its simple design, the complex conductance behaviour of our structure is not surprising: Due to the short length of the tiles, they are likely to partially unbind due to the electric field.[11] At the same time, the four duplexes are not connected at one end (see Figure 1 B), allowing for additional fluctuation. Potentially, the membrane bending we observed in the confocal images (see Figure 2 D) could be an alternative and highly interesting explanation for the wide spread of conductances. We believe that current traces with voltage-switching behaviour are likely to originate from DNA-tile structures that penetrate the membrane. For larger pores exhibiting similar behaviour, this orientation has been confirmed by PEG-sizing experiments.[14] However, a high membrane curvature could also induce ion conduction due to flexoelectricity.[27,28] On a related note, the DNA-tile structures could be catalysts for the formation of lipid pores as has been proposed for membrane proteins.[27] With this work, we shift the focus to smaller, highly flexible artificial ion channels constructed from DNA, whereas previous DNA membrane structures were preliminary designed for biosensing.[11,14]

In this study we showcase the versatility of DNA nanotechnology by diversifying the design of membrane-inserted DNA structures beyond the archetypal six-helix bundle. We show that DNA-tile assembly can be used to create ion-conducting structures with diameters comparable to biological ion channels within minutes. Ionic current recordings on lipid nano bilayers demonstrate that our DNA-tile assemblies exhibit multiple conductance states reminiscent of gating observed for biological ion channels. Due to the simple design with defined geometry, we expect that our work on DNA pores with near molecular inner diameters will help to understand gating and voltage-induced switching behaviour of DNA-based

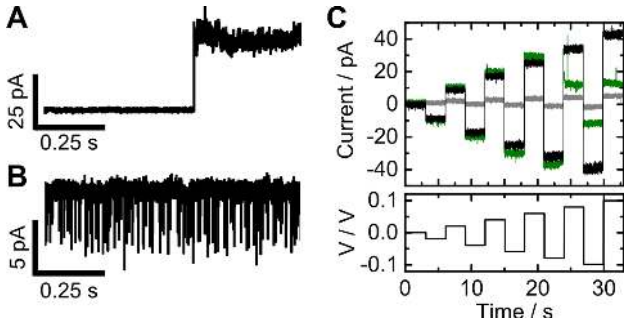

Figure 4: Characteristic events indicating the presence of a DNA-tile structure in the membrane include (A) insertion steps and (B) gating. C) Typical current traces obtained from an IV-recording in the presence of DNA-tile structures with cholesterol-anchors. Traces corresponding to plain bilayers (grey), ohmic traces (black) and traces with reduced conductance at higher voltage (green) are observed repeatedly.

membrane pores. Eventually this will guide the creation of man-made ion channels with controlled ion-selectivity and stimuli response.

Materials and Methods

Design and assembly of the DNA-tile structure. The structure was designed and visualised using the open source plug-in caDNAno.[29] Eight single-stranded DNA tiles (Integrated DNA Technologies, Inc.) were arranged on a square lattice to form a bundle of four interconnected DNA duplexes. Random sequences with non-sticky ends[17] were assigned to four tiles and complementary sequences were generated for the remaining (see SI, Table S1). One, two or four strands were selected for cholesterol modifications, two others carried Cy3-tags. For assembly of the DNA-tile structure, an equimolar mixture (1 μM in 10 mM Tris-HCl, 1 mM EDTA, 20 mM $MgCl_2$, pH 8.0) of the unmodified strands were annealed using a standard protocol (heating to 80 °C for 5 min, cooling down to 65 °C using a linear cooling ramp over 75 min, subsequently cooling to 25 °C within 16 h in a thermocycler (BioRad)). Alternatively, rapid assembly protocols were used as described in the text. The cholesterol-modified strands (Integrated DNA Technologies, Inc.) were added in 5× excess before each experiment.

Characterisation via AFM imaging, polyacrylamide gel electrophoresis and UV-melting. 5 μL of DNA-tile structures at a concentration of 100 nM in 10 mM Tris-HCl, 1 mM EDTA, 20 mM $MgCl_2$ was deposited on freshly cleaved mica and left for one minute to adsorb. The sample was then rinsed several times with ddH_2O to remove salts and dried with gaseous nitrogen. Imaging was performed using a Nanosurf Mobile S AFM in tapping mode. The DNA-tile structures were further characterised using 10% polyacrylamide gel electrophoresis in a solution containing 11 mM $MgCl_2$ buffered to approximately pH 8.3 with 45 mM Tris-borate, 1 mM EDTA and running conditions of 100 V and 90 min. Bands were stained with GelRed and visualised using UV-transilluminaton. For UV-melting experiments, 500 nM of the DNA-tile structure were added to a quartz cuvette (Sigma Aldrich) either in presence or in absence of lipid vesicles. The mixture was subjected to heating and cooling cycles (25 °C to 80 °C) at a rate of 5 °C/min in a Varian Cary 300 Bio UV/Vis spectrophotometer while monitoring the absorption at 260 nm.

Lipid vesicle preparation. 1,2-Diphytanoyl-sn-glycero-3-phosphatidylcholine (DPhPC; Avanti Polar Lipids), 10% cholesterol (Sigma Aldrich) giant unilamellar vesicles (GUVs) were prepared via electroformation using the Vesicle Prep Pro unit (Nanion technologies) and a protocol as previously described.[12] For the confocal imaging, 1,2-Dioleoyl-sn-glycero-3-phosphocholine (DOPC; Avanti Polar Lipids), or DOPC supplemented with 1% NBD-DPhPE, was used following the same procedure.

Fluorescent imaging. Cy3-labelled DNA-tile structures were added to GUVs and diluted to a final concentration of 100 nM (unless stated otherwise) in 10 mM Tris-HCl, 1 mM EDTA, 20 mM $MgCl_2$, pH 8.0 in an incubation chamber (Grace Biolabs). Imaging was performed using a Confocal Leica TCS SP5 microscope. Pores were excited at 514 nm using an Argon and a HeNe594 laser. Fluorescence emission was collected above 530 nm. Images were processed using ImageJ.

Single-channel recordings on the lipid nano bilayer setup. DNA-tile structures were incubated with GUVs at RT for 5 min and diluted to a final concentration of 50 nM in 1 M

KCl, 10 mM MES, pH 6.0. Bilayers were formed by suctioning the GUVs onto nano capillaries as previously described.[12] Each bilayer was subjected to a 33-second IV-recording at a sampling rate of 10 kHz. Current data was acquired using an Axopatch 200B amplifier and filtered at 2 kHz.

Acknowledgement

The authors thank Michael Walker and Elisa Hemming for critical reading of the manuscript. K.G. acknowledges funding from the Winton Programme for the Physics of Sustainability, Gates Cambridge and the Oppenheimer PhD studentship. T.Z. and A.E.C.M. acknowledge funding from the ERASMUS programme and S.H.A. from a Herchel Smith postdoctoral fellowship. S.K. and T.L. acknowledge funding from the DFG Nanosystems Initiative Munich. U.F.K. acknowledges funding from an ERC starting grant Passmembrane 261101 and Oxford Nanopore Technologies.

Supporting Information Available

A table with the utilised DNA sequences, dynamic light scattering (DLS) traces, UV-melting curves, extensive confocal fluorescent imaging studies, a table with results of further current recordings, exemplary current traces and a cost- and time estimation for the creation of DNA-tile structures.

This material is available free of charge via the Internet at `http://pubs.acs.org/`.

References

(1) Alberts, B.; Johnson, A.; Lewis, J.; Raff, M.; Roberts, K.; Walter, P. Molecular Biology of the Cell. 2002; `http://www.ncbi.nlm.nih.gov/books/NBK21054/`.

(2) Sakai, N.; Matile, S. *Langmuir* **2013**, *29*, 9031–9040.

(3) Kennedy, S. J.; Roeske, R. W.; Freeman, A. R.; Watanabe, A. M.; Besche, H. R. *Science* **1977**, *196*, 1341–2.

(4) Boccalon, M.; Iengo, E.; Tecilla, P. *J. Am. Chem. Soc.* **2012**, *134*, 20310–3.

(5) Clarke, J.; Wu, H.-C.; Jayasinghe, L.; Patel, A.; Reid, S.; Bayley, H. *Nat. Nanotechnol.* **2009**, *4*, 265–70.

(6) Burns, J. R.; Al-Juffali, N.; Janes, S. M.; Howorka, S. *Angew. Chem. Int. Ed.* **2014**, *53*, 12466–12470.

(7) Hernández-Ainsa, S.; Keyser, U. F. *Nanomedicine* **2013**, *8*, 1551–4.

(8) Bell, N. A. W.; Engst, C. R.; Ablay, M.; Divitini, G.; Ducati, C.; Liedl, T.; Keyser, U. F. *Nano Lett.* **2012**, *12*, 512–7.

(9) Hernández-Ainsa, S.; Bell, N. A. W.; Thacker, V. V.; Göpfrich, K.; Misiunas, K.; Fuentes-Perez, M. E.; Moreno-Herrero, F.; Keyser, U. F. *ACS Nano* **2013**, *7*, 6024–6030.

(10) Wei, R.; Martin, T. G.; Rant, U.; Dietz, H. *Angew. Chem. Int. Ed.* **2012**, *51*, 4864–7.

(11) Langecker, M.; Arnaut, V.; Martin, T. G.; List, J.; Renner, S.; Mayer, M.; Dietz, H.; Simmel, F. C. *Science* **2012**, *338*, 932–936.

(12) Burns, J. R.; Göpfrich, K.; Wood, J. W.; Thacker, V. V.; Stulz, E.; Keyser, U. F.; Howorka, S. *Angew. Chem. Int. Ed.* **2013**, *52*, 12069–72.

(13) Burns, J. R.; Stulz, E.; Howorka, S. *Nano Lett.* **2013**, *13*, 2351–2356.

(14) Seifert, A.; Göpfrich, K.; Burns, J. R.; Fertig, N.; Keyser, U. F.; Howorka, S. *ACS Nano* **2014**,

(15) Rothemund, P. W. K. *Nature* **2006**, *440*, 297–302.

(16) Wei, B.; Dai, M.; Yin, P. *Nature* **2012**, *485*, 623–6.

(17) Yin, P.; Hariadi, R. F.; Sahu, S.; Choi, H. M. T.; Park, S. H.; Labean, T. H.; Reif, J. H. *Science* **2008**, *321*, 824–6.

(18) Hernández-Ainsa, S.; Keyser, U. F. *Nanoscale* **2014**, *6*, 14121–32.

(19) Stachowiak, J. C.; Schmid, E. M.; Ryan, C. J.; Ann, H. S.; Sasaki, D. Y.; Sherman, M. B.; Geissler, P. L.; Fletcher, D. A.; Hayden, C. C. *Nat. Cell Biol.* **2012**, *14*, 944–9.

(20) Ford, M. G. J.; Mills, I. G.; Peter, B. J.; Vallis, Y.; Praefcke, G. J. K.; Evans, P. R.; McMahon, H. T. *Nature* **2002**, *419*, 361–6.

(21) Gornall, J. L.; Mahendran, K. R.; Pambos, O. J.; Steinbock, L. J.; Otto, O.; Chimerel, C.; Winterhalter, M.; Keyser, U. F. *Nano Lett.* **2011**, *11*, 3334–40.

(22) Göpfrich, K.; Kulkarni, C. V.; Pambos, O. J.; Keyser, U. F. *Langmuir* **2013**, *29*, 355–364.

(23) Mandelkern, M.; Elias, J. G.; Eden, D.; Crothers, D. M. *J. Mol. Biol.* **1981**, *152*, 153–161.

(24) Ke, Y.; Douglas, S. M.; Liu, M.; Sharma, J.; Cheng, A.; Leung, A.; Liu, Y.; Shih, W. M.; Yan, H. *J. Am. Chem. Soc.* **2009**, *131*, 15903–15908.

(25) Schiffels, D.; Liedl, T.; Fygenson, D. K. *ACS Nano* **2013**, *7*, 6700–6710.

(26) Bai, X.-C.; Martin, T. G.; Scheres, S. H. W.; Dietz, H. *Proc. Natl. Acad. Sci. U.S.A.* **2012**, *109*, 20012–7.

(27) Mosgaard, L. D.; Heimburg, T. *Acc. Chem. Res.* **2013**, *46*, 2966–76.

(28) Petrov, A. *Physical and chemical basis of information transfer*; 1975; pp 111–125.

(29) Douglas, S. M.; Marblestone, A. H.; Teerapittayanon, S.; Vazquez, A.; Church, G. M.; Shih, W. M. *Nucleic Acids Res.* **2009**, *37*, 5001–6.

Graphical TOC Entry

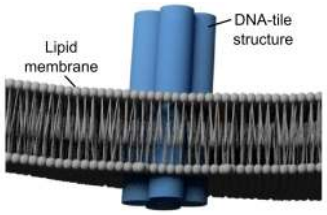

Illustration of the ion-channel like DNA-tile structure embedded into a lipid membrane.